ORGANOMETALLICS

pubs.acs.org/Organometallics

Communication

Reductive Elimination from Sterically Encumbered Ni–Polypyridine Complexes

Craig S. Day, Stephanie J. Ton,[⊥] Ryan T. McGuire,[⊥] Cina Foroutan-Nejad,* and Ruben Martin*

Cite This: *Organometallics* 2022, 41, 2662–2667

Read Online

ACCESS | Metrics & More | Article Recommendations | Supporting Information

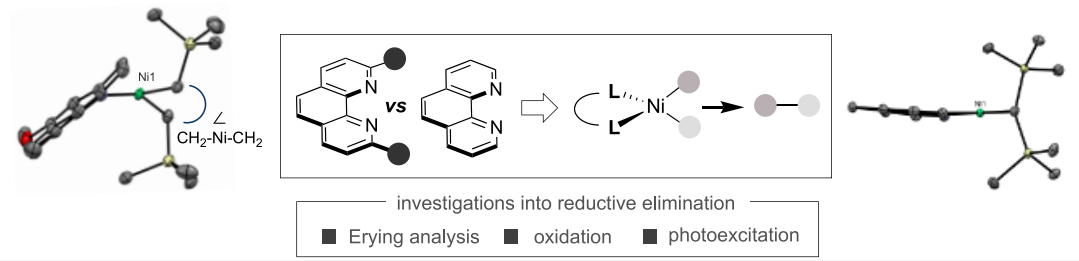

ABSTRACT: Herein we disclose the synthesis of sterically encumbered dialkylnickel(II) complexes bearing 2,9-dimethyl-1,10-phenanthroline ligands. A comparison with their unsubstituted analogues by both X-ray crystallography and theoretical calculations revealed significant distortions in their molecular structures. Eyring plots along with stoichiometric and photoexcitation studies revealed that sterically encumbered dialkylnickel(II) complexes enable facile C(sp^3)–C(sp^3) reductive elimination, thus offering an improved understanding of Ni catalysis.

Nickel-catalyzed reactions have gained considerable momentum as enabling techniques for forging new synthetic architectures.[1−4] Particularly attractive is the virtue of Ni catalysts for forging C(sp^3)–C(sp^3) bonds, as these bonds are key motifs in medicinal chemistry programs that modulate solubility, molecular shape, or substrate recognition of drug candidates.[5−8] The successful implementation of nickel catalysis in both academic and industrial laboratories is intimately associated with the ease of enabling single-electron-transfer reactivity, the propensity to populate unconventional Ni(I) or Ni(III) manifolds, and the high barrier for β-hydride elimination that allows for forging of sp^3 architectures.[9] Reviewing the literature data reveals that sterically encumbered polypyridine ligands have proved to be a key contributory factor for success in a myriad of Ni-catalyzed C(sp^3)–C(sp^3) bond formations.[10] Although there exists a reasonable consensus on how Ni–polypyridine complexes enable oxidative addition or transmetalation, the means to trigger C(sp^3)–C(sp^3) reductive elimination remains the subject of considerable debate due to the inherent difficulty of accessing short-lived yet exceptionally sensitive dialkylnickel(II)–polypyridine species (Scheme 1, top).[11−18] Seminal studies by Yamamoto et al. determined that the barrier to reductive elimination from (bpy)$NiEt_2$ was 68 kcal·mol^{-1}.[19−24] The extensive literature on the steric implications of phosphine ligands for reductive elimination and the rapid adoption of sterically encumbered polypyridine ligands for the construction of C(sp^3)–C(sp^3) bonds prompted our interest in studying these systems further (Scheme 1, middle).[25,26] We anticipated that a study aimed at unraveling the steric effects of dialkylnickel–polypyridine complexes on C(sp^3)–C(sp^3) reductive elimination might represent a new lead for future Ni-catalyzed cross-coupling reactions (Scheme 1, bottom).

We began our investigations by synthesizing well-defined dialkylnickel(II) complexes bearing variously substituted polypyridine ligands.[21] Specifically, we allowed $Ni(acac)_2$ to react with Et_2AlOEt in the presence of either 2,2′-bipyridine (**L1**) or neocuproine (**L2**) in Et_2O at −20 °C (Figure 1). While the synthesis of (**L1**)$NiEt_2$ (**1**) posed no problems, the preparation of (**L2**)$NiEt_2$ was found to be particularly problematic, as (**L2**)Ni(ethylene) crystallized from the reaction mixture in 60% yield. This product, corroborated by X-ray diffraction, presumably arises from β-hydride elimination. The exceptional ease with which (**L2**)$NiEt_2$ undergoes β-hydride elimination is in sharp contrast with the high barrier observed in the analogous reaction of (**L1**)$NiEt_2$. The importance of this observation can hardly be overestimated, as it offers indirect yet long-awaited evidence for the propensity of 2,9-disubstituted phenanthroline to enable Ni-catalyzed chain walking via iterative β-hydride elimination and migratory insertion events.[27]

Received: July 21, 2022
Published: September 21, 2022

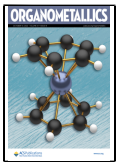

https://doi.org/10.1021/acs.organomet.2c00362
Organometallics 2022, 41, 2662–2667

Scheme 1. Reductive Elimination of Polypyridine-Ligated Ni Complexes

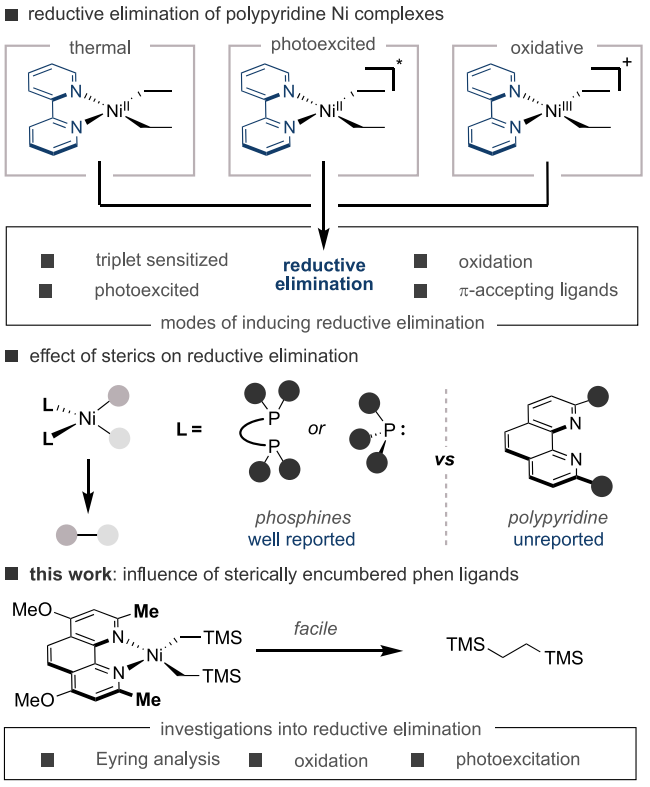

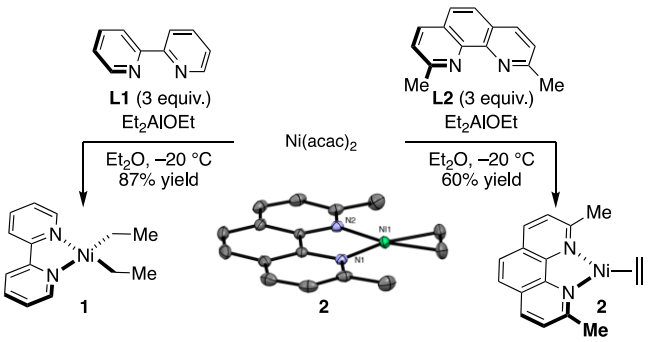

Figure 1. Initial efforts en route to dialkylnickel(II) species.

Aiming to understand the factors influencing reductive elimination of Ni(dialkyl) complexes supported by sterically encumbered polypyridine ligands and the difficulties of synthesizing L_2NiR_2 complexes by the use of alkylaluminum reagents, we sought out a pathway involving neutral ligand displacement. To this end, we turned our attention to $(py)_2Ni(CH_2TMS)_2$ (TMS = trimethylsilyl), which is easily prepared by reaction of $(py)_4NiCl_2$ with $TMSCH_2MgCl$ in Et_2O at −60 °C.[28] This nickel precursor was chosen because of the ease with which monodentate pyridine ligands could be displaced by 1,10-phenanthroline ligands. Furthermore, we anticipated that the CH_2TMS groups would add to the stability of the complexes by hyperconjugation and by preventing β-hydride elimination.[29−32] As expected from early studies reported by Carmona and Atwood, (**L3**)$Ni(CH_2TMS)_2$ (**3**) was prepared in 90% yield by the reaction between $(py)_2Ni(CH_2TMS)_2$ and 1,10-phenanthroline (**L3**) at room temperature.[28] Notably, the reaction between $(py)_2Ni(CH_2TMS)_2$ and 4,7-dimethoxy-2,9-dimethyl-1,10-phenanthroline (**L4**)—a ligand featuring electron-donating methoxy groups via resonance donation to the ligand π system—could be conducted at −36 °C, giving rise to (**L4**)$Ni(CH_2TMS)_2$ (**4**) in 68% yield as a purple solid (Figure 2). The stability of this

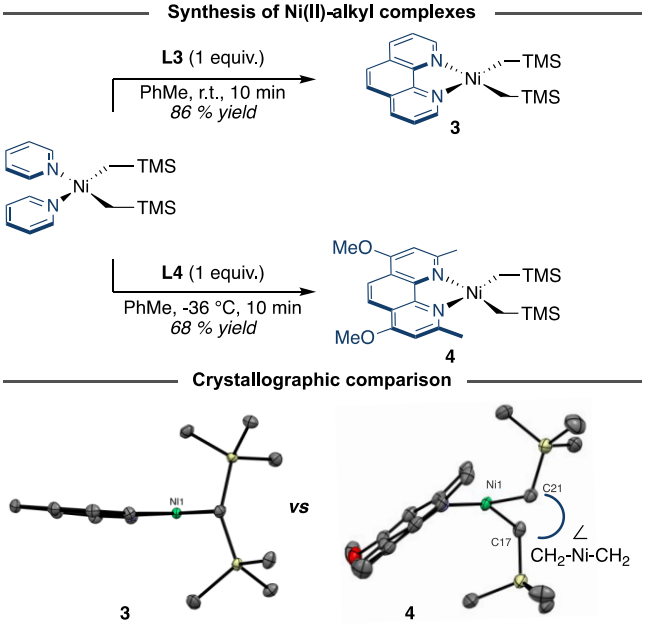

Figure 2. Synthesis of (**L**)$Ni(CH_2TMS)_2$ (**L** = **L3**, **L4**) and ORTEP drawings (50%) of **3** and **4**. Crystals of **3** and **4** were grown at −36 °C in Et_2O/pentane or Et_2O. Hydrogen atoms and disordered sections have been omitted in the sake of clarity.

complex may arise from the electron-richness of the metal center, which prevents reductive elimination. In keeping with this hypothesis, not even traces of (**L5**)$Ni(CH_2TMS)_2$ (**L5** = 2,9-dimethyl-4,7-diphenyl-1,10-phenanthroline) were observed upon the reaction of $(py)_2Ni(CH_2TMS)_2$ with **L5**, a ligand with inductively withdrawing phenyl groups in place of the methoxy groups of **L4**. The preparation of **4** is particularly important, as it offers for the first time the opportunity to assess the influence of sterically encumbered polypyridine complexes in the context of $C(sp^3)-C(sp^3)$ reductive elimination from a well-defined species. This information may therefore allow the parametrization of features that may have an impact in future Ni-catalyzed endeavors.

Low-temperature crystallization (−36 °C, Et_2O/pentane or Et_2O) furnished crystals suitable for X-ray diffraction, thus allowing the structures of **3** and **4** to be determined unambiguously. A simple comparison of their structures is particularly illustrative. While the Ni atom in **3** is in a canonical square planar geometry, the bonding in **4** is fairly distorted from a square planar geometry, although the complex is still diamagnetic. DFT calculations of the gas-phase structure of **4** confirmed that this nonplanarity is a molecular phenomenon, not a result of the crystal packing. Strikingly, the coordination of **L4** is ligated at a ca. 35° angle, which results in poor overlap of the σ-sp^2 orbital of nitrogen with the central Ni atom. This is reflected in lower values of the delocalization index δ(A, B)—a measure of the orbital overlap and covalent bond order between a pair of atoms A and B—computed within the context of the quantum theory of atoms in molecules (QTAIM):[33] in **4**, δ(Ni, N) = 0.459 and 0.394, whereas in

https://doi.org/10.1021/acs.organomet.2c00362
Organometallics 2022, 41, 2662−2667

3, δ(Ni, N) = 0.499. Natural bond orbital analysis further confirmed a weaker overlap between the lone pairs of the nitrogen atoms and the p orbital of Ni in **4**. While second-order perturbation theory for the symmetrical structure of **3** predicted two equally strong interactions from the nitrogen atoms of **L3** ($E(2)$ = 35.2 kcal·mol^{-1}), a significant deviation is observed in nonsymmetrical **L4** ($E(2)$ = 33.6 and 33.9 kcal·mol^{-1}). We speculate that this indirect binding mode might limit steric pressure surrounding the Ni center, as a direct binding interaction might locate the 2,9-dimethyl substituents of **L4** in close proximity to the methylene carbons on the CH_2TMS moiety.

Further inspection of the X-ray structure of **4** identified a heavily distorted square planar geometry, with the methylene carbon C17 significantly out of the N1−Ni−N2 plane. A seemingly simple comparison of the CH_2−Ni−CH_2 angle from the side as shown in Figure 2 reveals that the methylene carbons are distorted by 38.9°, which is in contrast to the distortion of 2.8° observed for **3**. Further comparison of the two structures revealed that **4** has longer N−Ni bonds (2.055(3) and 1.982(3) Å in **4** vs 1.9833(16) and 1.9886(15) in **3**) and contracted Ni−C linkages (1.930(3) and 1.933(3) Å in **4** vs 1.9441(18) and 1.9442(18) Å in **3**). Comparing the QTAIM atomic charges (q(Ni)) and localization index (λ(Ni)) of **3** and **4** suggests that **L4** in **4** increases the electron population of Ni more than does coordination of **L3** in **3** ($q(\mathrm{Ni})_4$ = +0.612 and $\lambda(\mathrm{Ni})_4$ = 25.755 vs $q(\mathrm{Ni})_3$ = +0.635 and $\lambda(\mathrm{Ni})_3$ = 25.699). Analysis of the frontier molecular orbitals of **3** and **4** reveals that the complexation with **L4** increases the HOMO energies of **4** more than those of **3** (Figure 3), which is consistent with the highly strained geometry of **4**. Consistent with **4** containing a higher-energy HOMO were cyclic voltammetry experiments which found that Ni(II/III) oxidation is easier in **4** (E_{ox} = −0.40 V vs SCE) than in **3** (E_{ox} = 0.22 V vs SCE).

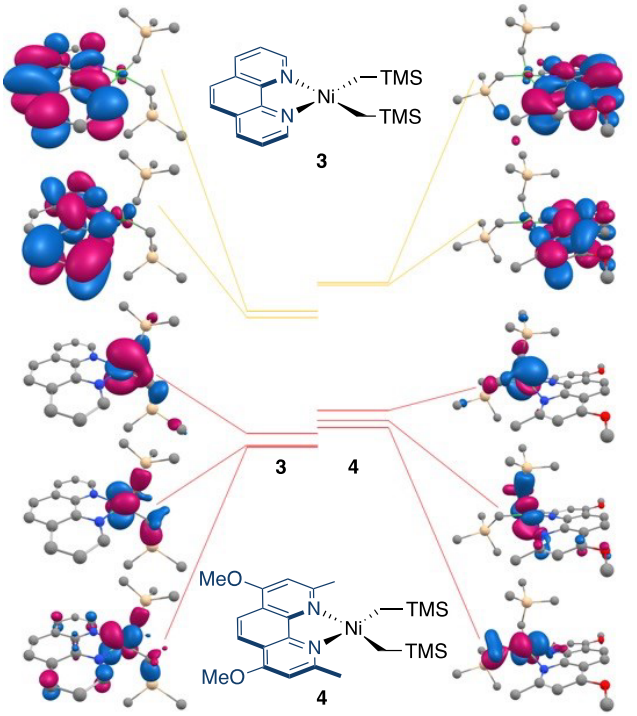

Figure 3. Frontier molecular orbitals of (left) **3** and (right) **4** by DFT.

In order to study the ligand effects of **L3** and **L4** on C−C reductive elimination from **3** and **4**, respectively, we monitored these compounds at elevated temperature in C_6D_6. Demonstrating the stability of **3**, even after 24 h at 100 °C, **3** showed no reaction. The striking stability of **3** is in sharp contrast to its sterically encumbered analogue **4**, which underwent reductive elimination in C_6D_6 at 60 °C with a first-order decay (k = 3.72 × 10^{-4} s^{-1}) over 100 min to form insoluble $(\mathbf{L4})_2$Ni and 1,2-bis(trimethylsilyl)ethane (Figure 4).

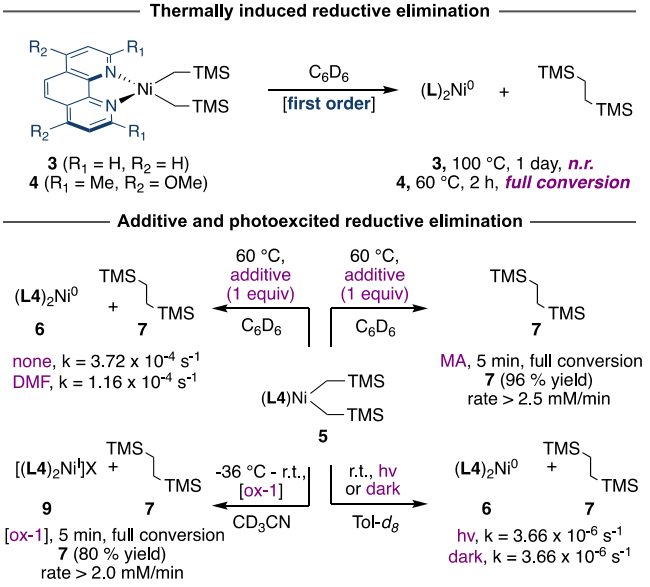

Figure 4. Reductive elimination of $TMSCH_2CH_2TMS$ from **4** under various conditions: thermally, with additives, under ambient light and with an oxidant. ox-1 = 1-fluoro-2,4,6-trimethylpyridinium tetrafluoroborate.

Further information on the reductive elimination was gathered by performing an Eyring analysis in C_6D_6, which determined a particularly low activation barrier ($\Delta G^{\ddagger}$(50 °C) = 26.3 kcal·mol^{-1}). Qualitative data on the transition state could be obtained by performing a preliminary three-point Eyring plot analysis in THF-d_8 (50−70 °C) with single kinetic runs, from which a negative entropy of activation is apparent (Figure S11).[34] To gain additional information on the effect of coordinating ligands, we examined whether the inclusion of methyl acrylate (MA) might influence reductive elimination in **4**. In line with studies performed by Yamamoto with (bpy)$NiEt_2$, the presence of the π-accepting olefin MA induced rapid reductive elimination (<5 min), which we speculate is due to the intermediacy of five-coordinate species via interaction with the $d_{x^2-y^2}$ orbital (Figure 4).[35] Taking into consideration that metallaphotoredox scenarios have gained considerable momentum as innovative vehicles for forging sp^3 architectures, we next focused our attention on studying whether C(sp^3)−C(sp^3) reductive elimination of **4** might be facilitated by either photoexcitation or single-electron-transfer oxidation. Notably, a rate enhancement similar to that observed for MA was observed when the reaction of **4** was conducted with 1-fluoro-2,4,6-trimethylpyridinium tetrafluoroborate, which acts as a one-electron oxidant,[36] thus illustrating the exceptional ease with which Ni(III) inter-

https://doi.org/10.1021/acs.organomet.2c00362
Organometallics 2022, 41, 2662−2667

mediates promote reductive elimination. Comparing the rate of reductive elimination of **4** in the dark or under ambient light (**4** absorbs (λ_{max} = 399 nm)) revealed a similar rate of reaction (k = 3.66 × $10^{-6}s^{-1}$).[37] These observations were further corroborated by the lack of changes in the crystal structure of **4** when crystals of **4** were irradiated at 390 nm.

In summary, we have reported the first dialkylnickel(II) complex supported by sterically encumbered 2,9-disubstituted phenanthroline ligands. A comparison of the solid-state geometry with that of its unsubstituted analogue reveals that steric effects destabilize these complexes, setting the basis for promoting C(sp^3)−C(sp^3) reductive elimination with exceptional ease. Stoichiometric experiments were carried out in different solvents, in the presence of additives, and in the presence of light. We believe that this report might lead to new knowledge in synthetic design while offering a new gateway for studying the intricacies of Ni-catalyzed reactions.

■ ASSOCIATED CONTENT

Supporting Information

The Supporting Information is available free of charge at https://pubs.acs.org/doi/10.1021/acs.organomet.2c00362.

Cartesian coordinates for **3** (XYZ)

Cartesian coordinates for **4** (XYZ)

Experimental procedures and spectral and crystallographic data (PDF)

Accession Codes

CCDC 2191651−2191654 contain the supplementary crystallographic data for this paper. These data can be obtained free of charge via www.ccdc.cam.ac.uk/data_request/cif, or by emailing data_request@ccdc.cam.ac.uk, or by contacting The Cambridge Crystallographic Data Centre, 12 Union Road, Cambridge CB2 1EZ, U.K.; fax: +44 1223 336033.

■ AUTHOR INFORMATION

Corresponding Authors

Ruben Martin − *The Barcelona Institute of Science and Technology, Institute of Chemical Research of Catalonia (ICIQ), 43007 Tarragona, Spain; ICREA, 08010 Barcelona, Spain;* orcid.org/0000-0002-2543-0221; Email: rmartinromo@iciq.es

Cina Foroutan-Nejad − *Institute of Organic Chemistry, Polish Academy of Sciences, 01-224 Warsaw, Poland;* Email: cforoutan-nejad@icho.edu.pl

Authors

Craig S. Day − *The Barcelona Institute of Science and Technology, Institute of Chemical Research of Catalonia (ICIQ), 43007 Tarragona, Spain; Departament de Química Analítica i Química Orgànica, Universitat Rovira i Virgili, 43007 Tarragona, Spain;* orcid.org/0000-0002-6931-0280

Stephanie J. Ton − *The Barcelona Institute of Science and Technology, Institute of Chemical Research of Catalonia (ICIQ), 43007 Tarragona, Spain*

Ryan T. McGuire − *The Barcelona Institute of Science and Technology, Institute of Chemical Research of Catalonia (ICIQ), 43007 Tarragona, Spain*

Complete contact information is available at: https://pubs.acs.org/10.1021/acs.organomet.2c00362

Author Contributions

[⊥]S.J.T. and R.T.M. contributed equally to this work.

Notes

The authors declare no competing financial interest.

■ ACKNOWLEDGMENTS

We thank thank ICIQ and MICIU (PID2021-133801NB-I00) for financial support. C.S.D. thanks the European Union's Horizon 2020 Programme under Marie Curie PREBIST Grant Agreement 754558. C.F.N. thanks the National Science Centre, Poland (2020/39/B/ST4/02022) for partially funding this work. This research was supported in part by PLGrid Infrastructure. For Open Access, the authors have applied a CC-BY public copyright license to any Author Accepted Manuscript (AAM) version arising from this submission. We sincerely thank E. Escudero and J. Benet for X-ray crystallographic data.

■ REFERENCES

(1) Hazari, N.; Melvin, P. R.; Beromi, M. M. Well-defined nickel and palladium precatalysts for cross-coupling. *Nat. Rev. Chem.* **2017**, *1* (3), 0025.

(2) Tasker, S. Z.; Standley, E. A.; Jamison, T. F. Recent advances in homogeneous nickel catalysis. *Nature* **2014**, *509* (7500), 299−309.

(3) Diccianni, J.; Lin, Q.; Diao, T. Mechanisms of Nickel-Catalyzed Coupling Reactions and Applications in Alkene Functionalization. *Acc. Chem. Res.* **2020**, *53* (4), 906−919.

(4) Diccianni, J. B.; Diao, T. Mechanisms of Nickel-Catalyzed Cross-Coupling Reactions. *Trends Chem.* **2019**, *1* (9), 830−844.

(5) Choi, J.; Fu, G. C. Transition metal-catalyzed alkyl−alkyl bond formation: Another dimension in cross-coupling chemistry. *Science* **2017**, *356* (6334), No. eaaf7230.

(6) Burke, M. D.; Schreiber, S. L. A Planning Strategy for Diversity-Oriented Synthesis. *Angew. Chem., Int. Ed.* **2004**, *43* (1), 46−58.

(7) Lipinski, C.; Hopkins, A. Navigating chemical space for biology and medicine. *Nature* **2004**, *432* (7019), 855−861.

(8) Dombrowski, A. W.; Gesmundo, N. J.; Aguirre, A. L.; Sarris, K. A.; Young, J. M.; Bogdan, A. R.; Martin, M. C.; Gedeon, S.; Wang, Y. Expanding the Medicinal Chemist Toolbox: Comparing Seven C(sp^2)−C(sp^3) Cross-Coupling Methods by Library Synthesis. *ACS Med. Chem. Lett.* **2020**, *11* (4), 597−604.

(9) Chan, A. Y.; Perry, I. B.; Bissonnette, N. B.; Buksh, B. F.; Edwards, G. A.; Frye, L. I.; Garry, O. L.; Lavagnino, M. N.; Li, B. X.; Liang, Y.; Mao, E.; Millet, A.; Oakley, J. V.; Reed, N. L.; Sakai, H. A.; Seath, C. P.; MacMillan, D. W. C. Metallaphotoredox: The Merger of Photoredox and Transition Metal Catalysis. *Chem. Rev.* **2022**, *122* (2), 1485−1542.

(10) For selected references, see: (a) Sun, S.-Z.; Börjesson, M.; Martin-Montero, R.; Martin, R. Site-Selective Ni-Catalyzed Reductive Coupling of α-Haloboranes with Unactivated Olefins. *J. Am. Chem. Soc.* **2018**, *140* (40), 12765−12769. (b) Sun, S.-Z.; Romano, C.; Martin, R. Site-Selective Catalytic Deaminative Alkylation of Unactivated Olefins. *J. Am. Chem. Soc.* **2019**, *141* (41), 16197−16201. (c) Sun, S.-Z.; Talavera, L.; Spieß, P.; Day, C. S.; Martin, R. sp^3 Bis-Organometallic Reagents via Catalytic 1,1-Difunctionalization of Unactivated Olefins. *Angew. Chem., Int. Ed.* **2021**, *60* (21), 11740−11744. (d) Janssen-Müller, D.; Sahoo, B.; Sun, S.-Z.; Martin, R. Tackling Remote sp^3 C−H Functionalization via Ni-Catalyzed "chain-walking" Reactions. *Isr. J. Chem.* **2020**, *60* (3−4), 195−206. (e) Zhou, F.; Zhu, J.; Zhang, Y.; Zhu, S. NiH-Catalyzed Reductive Relay Hydroalkylation: A Strategy for the Remote C(sp^3)−H Alkylation of Alkenes. *Angew. Chem., Int. Ed.* **2018**, *57* (15), 4058−4062. (f) Wang, Z.; Yin, H.; Fu, G. C. Catalytic enantioconvergent coupling of secondary and tertiary electrophiles with olefins. *Nature* **2018**, *563* (7731), 379−383. (g) Zhou, F.; Zhang, Y.; Xu, X.; Zhu, S. NiH-Catalyzed Remote Asymmetric Hydroalkylation of Alkenes with

Racemic α-Bromo Amides. *Angew. Chem., Int. Ed.* **2019**, *58* (6), 1754−1758.
(11) Ju, L.; Hu, C. T.; Diao, T. Strategies for Promoting Reductive Elimination of Bi- and Bis-Oxazoline Ligated Organonickel Complexes. *Organometallics* **2022**, *41* (14), 1748−1753.
(12) Dong, Z.; MacMillan, D. W. C. Metallaphotoredox-enabled deoxygenative arylation of alcohols. *Nature* **2021**, *598* (7881), 451−456.
(13) Tian, L.; Till, N. A.; Kudisch, B.; MacMillan, D. W. C.; Scholes, G. D. Transient Absorption Spectroscopy Offers Mechanistic Insights for an Iridium/Nickel-Catalyzed C−O Coupling. *J. Am. Chem. Soc.* **2020**, *142* (10), 4555−4559.
(14) Kim, T.; McCarver, S. J.; Lee, C.; MacMillan, D. W. C. Sulfonamidation of Aryl and Heteroaryl Halides through Photosensitized Nickel Catalysis. *Angew. Chem., Int. Ed.* **2018**, *57* (13), 3488−3492.
(15) Twilton, J.; Le, C.; Zhang, P.; Shaw, M. H.; Evans, R. W.; MacMillan, D. W. C. The merger of transition metal and photocatalysis. *Nat. Rev. Chem.* **2017**, *1* (7), 0052.
(16) Welin, E. R.; Le, C.; Arias-Rotondo, D. M.; McCusker, J. K.; MacMillan, D. W. C. Photosensitized, energy transfer-mediated organometallic catalysis through electronically excited nickel(II). *Science* **2017**, *355* (6323), 380−385.
(17) Koo, K.; Hillhouse, G. L. Carbon-Nitrogen Bond Formation by Reductive Elimination from Nickel(II) Amido Alkyl Complexes. *Organometallics* **1995**, *14* (9), 4421−4423.
(18) Matsunaga, P. T.; Hess, C. R.; Hillhouse, G. L. Reactions of Organoazides with Nickel Alkyls. Syntheses and Reactions of Nickel(II) Amido Complexes. *J. Am. Chem. Soc.* **1994**, *116* (8), 3665−3666.
(19) Choi, B.-K.; Yamamoto, T. Electrochemical properties of new n-type π-conjugated polybipyridines and polybiphenylenes with various bridging units. *Electrochem. Commun.* **2003**, *5* (7), 566−570.
(20) Yamamoto, T. Synthesis of π-Conjugated Polymers Bearing Electronic and Optical Functionalities by Organometallic Polycondensations. Chemical Properties and Applications of the π-Conjugated Polymers. *Synlett* **2003**, *2003*, 425−450.
(21) Saito, T.; Uchida, Y.; Misono, A.; Yamamoto, A.; Morifuji, K.; Ikeda, S. Diethyldipyridylnickel. Preparation, Characterization, and Reactions. *J. Am. Chem. Soc.* **1966**, *88* (22), 5198−5201.
(22) Yamamoto, T.; Yamamoto, A.; Ikeda, S. Organo (dipyridyl) nickel complexes. I. Stability and activation of the alkyl-nickel bonds of dialkyl (dipyridyl) nickel by coordination with various substituted olefins. *J. Am. Chem. Soc.* **1971**, *93* (14), 3350−3359.
(23) Yamamoto, T.; Abla, M. Reductive elimination of Et—Et from $NiEt_2$(bpy) promoted by electron-accepting aromatic compounds. *J. Organomet. Chem.* **1997**, *535* (1), 209−211.
(24) Yamamoto, T.; Yamamoto, A.; Ikeda, S. Organo (dipyridyl) nickel complexes. II. Stabilities of olefin-nickel bonds in olefin-coordinated dipyridylnickel and dialkyl (dipyridyl) nickel complexes. *J. Am. Chem. Soc.* **1971**, *93* (14), 3360−3364.
(25) van Leeuwen, P. W. N. M.; Kamer, P. C. J.; Reek, J. N. H.; Dierkes, P. Ligand Bite Angle Effects in Metal-catalyzed C−C Bond Formation. *Chem. Rev.* **2000**, *100* (8), 2741−2770.
(26) Kohara, T.; Yamamoto, T.; Yamamoto, A. Ligand exchange reaction between $NiMe_2L_2$ (L = bpy, PEt_3) and ditertiary phosphines $Ph_2P(CH_2)_nPPh_2$ (n = 1−4) and effect of ligand on ease of reductive elimination of C_2H_6 from $NiMe_2(Ph_2P(CH_2)nPPh_2)$. *J. Organomet. Chem.* **1980**, *192* (2), 265−274.
(27) For selected examples in which 2,9-disubstituted polypyridine ligands promote chain walking, see ref 10d and the following references: (a) Juliá-Hernández, F.; Moragas, T.; Cornella, J.; Martin, R. Remote Carboxylation of Halogenated Aliphatic Hydrocarbons with Carbon Dioxide. *Nature* **2017**, *545* (7652), 84−88. (b) He, Y.; Cai, Y.; Zhu, S. Mild and Regioselective Benzylic C−H Functionalization: Ni-Catalyzed Reductive Arylation of Remote and Proximal Olefins. *J. Am. Chem. Soc.* **2017**, *139* (3), 1061−1064. (c) Wang, X.; Nakajima, M.; Serrano, E.; Martin, R. Alkyl Bromides as Mild Hydride Sources in Ni-Catalyzed Hydroamidation of Alkynes with Isocyanates. *J. Am. Chem. Soc.* **2016**, *138* (48), 15531−15534. (d) Chen, F.; Chen, K.; Zhang, Y.; He, Y.; Wang, Y.-M.; Zhu, S. Remote Migratory Cross-Electrophile Coupling and Olefin Hydroarylation Reactions Enabled by in Situ Generation of NiH. *J. Am. Chem. Soc.* **2017**, *139* (39), 13929−13935. (e) Tortajada, A.; Juliá-Hernández, F.; Börjesson, M.; Moragas, T.; Martin, R. Transition-Metal-Catalyzed Carboxylation Reactions with Carbon Dioxide. *Angew. Chem., Int. Ed.* **2018**, *57* (49), 15948−15982. (f) Tortajada, A.; Menezes Correia, J. T.; Serrano, E.; Monleón, A.; Tampieri, A.; Day, C. S.; Juliá-Hernández, F.; Martin, R. Ligand-Controlled Regiodivergent Catalytic Amidation of Unactivated Secondary Alkyl Bromides. *ACS Catal.* **2021**, *11* (16), 10223−10227. (g) Li, Y.; Luo, Y.; Peng, L.; Li, Y.; Zhao, B.; Wang, W.; Pang, H.; Deng, Y.; Bai, R.; Lan, Y.; Yin, G. Reaction scope and mechanistic insights of nickel-catalyzed migratory Suzuki−Miyaura cross-coupling. *Nat. Commun.* **2020**, *11* (1), 417. (h) Peng, L.; Li, Z.; Yin, G. Photochemical Nickel-Catalyzed Reductive Migratory Cross-Coupling of Alkyl Bromides with Aryl Bromides. *Org. Lett.* **2018**, *20* (7), 1880−1883. (i) Peng, L.; Li, Y.; Li, Y.; Wang, W.; Pang, H.; Yin, G. Ligand-Controlled Nickel-Catalyzed Reductive Relay Cross-Coupling of Alkyl Bromides and Aryl Bromides. *ACS Catal.* **2018**, *8* (1), 310−313.
(28) Carmona, E.; González, F.; Poveda, M. L.; Atwood, J. L.; Rogers, R. D. Synthesis and properties of dialkyl complexes of nickel(II). The crystal structure of bis(pyridine)bis-(trimethylsilylmethyl)nickel(II). *J. Chem. Soc., Dalton Trans.* **1981**, No. 3, 777−782.
(29) Kapadia, R.; Brian Pedley, J.; Brent Young, G. Relative metal-carbon bond enthalpies and trans-influences for neopoentylplatinum-(II) and trimethysilylmethylplatinum(II) complexes: an unusual case of weaker M-C binding by a β-silylmethyl ligand than its carbon analogue. *Inorg. Chim. Acta* **1997**, *265* (1), 235−239.
(30) Lappert, M. F.; Patil, D. S.; Pedley, J. B. Standard heats of formation and M−C bond energy terms for some homoleptic transition metal alkyls MR. *J. Chem. Soc., Chem. Commun.* **1975**, No. 20, 830−831.
(31) Fendrick, C. M.; Marks, T. J. Thermochemically based strategies for carbon-hydrogen activation on saturated hydrocarbon molecules. Ring-opening reactions of a thoracyclobutane with tetramethylsilane and methane. *J. Am. Chem. Soc.* **1984**, *106* (7), 2214−2216.
(32) Sjoegren, M.; Hansson, S.; Norrby, P. O.; Aakermark, B.; Cucciolito, M. E.; Vitagliano, A. Selective stabilization of the anti isomer of (η^3-allyl) palladium and-platinum complexes. *Organometallics* **1992**, *11* (12), 3954−3964.
(33) Bader, R. F. W. *Atoms in Molecules: A Quantum Theory*; Clarendon Press: Oxford, U.K., 1990.
(34) Quantification of 1,2-bis(trimethylsilyl)ethane from the crude reaction mixture in C_6D_6 at 60 °C showed that this product was formed in 51% yield. While we were unable to determine the side products formed, possibly paramagnetic species with ligand C−H activation are generated. For a recent example, see: Davies, J.; Janssen-Müller, D.; Zimin, D. P.; Day, C. S.; Yanagi, T.; Elfert, J.; Martin, R. Ni-Catalyzed Carboxylation of Aziridines en Route to β-Amino Acids. *J. Am. Chem. Soc.* **2021**, *143* (13), 4949−4954.
(35) Monitoring the reductive elimination of **5** at 60 °C in C_6D_6 with 1 equiv of DMF revealed a slight reduction in rate (k = 1.16 × 10−4 s^{-1}). We tentatively attribute this to the increase in the polarity of the solution, as an increase in solvent polarity may destabilize a nonpolar transition state.
(36) For the use of 1-fluoro-2,4,6-trimethylpyridinium tetrafluoroborate as a single-electron oxidant, see: (a) Shevick, S. L.; Obradors, C.; Shenvi, R. A. Mechanistic Interrogation of Co/Ni-Dual Catalyzed Hydroarylation. *J. Am. Chem. Soc.* **2018**, *140* (38), 12056−12068. (b) Kiselyov, A. S. Chemistry of N-fluoropyridinium salts. *Chem. Soc. Rev.* **2005**, *34* (12), 1031−1037.
(37) Experiments with Kessil irradition resulted in a significant rate increase, which we attribute to heating from the lamp. For examples in which ambient light promoted the rate of reaction see: (a) Boudjelel, M.; Riedel, R.; Schrock, R. R.; Conley, M. P.; Berges, A. J.; Carta, V.

https://doi.org/10.1021/acs.organomet.2c00362
Organometallics 2022, 41, 2662−2667

Tungstacyclopentane Ring Contraction Yields Olefin Metathesis Catalysts. *J. Am. Chem. Soc.* **2022**, *144* (24), 10929−10942. (b) Day, C. S.; Fogg, D. E. High-Yield Synthesis of a Long-Sought, Labile Ru-NHC Complex and Its Application to the Concise Synthesis of Second-Generation Olefin Metathesis Catalysts. *Organometallics* **2018**, *37* (24), 4551−4555.

https://doi.org/10.1021/acs.organomet.2c00362
Organometallics 2022, 41, 2662−2667